Journal of the Serbian Chemical Society
JSCS-info@shd.org.rs • www.shd.org.rs/JSCS
J. Serb. Chem. Soc. *86* (9) 845–857 (2021)
JSCS–5466
Original scientific paper
Published 27 May, 2021

Fluoride ion conductivity of solid solutions $K_xPb_{0.86-x}Sn_{1.14}F_{4-x}$

YULIIA POHORENKO[1]*, ROMAN PSHENYCHNYI[2], TAMARA PAVLENKO[1], ANATOLIY OMEL'CHUK[1] and VOLODYMYR TRACHEVSKYI[3]

[1]V.I. Vernadskii Institute of General and Inorganic Chemistry of the Ukrainian NAS, 32–34 Acad. Palladina Ave., 03142 Kyiv, Ukraine, [2]Sumy State University, Rymskogo-Korsakova st. 2, 40007 Sumy, Ukraine and [3]G.V. Kurdyumov Institute of Metal Physics of the Ukrainian NAS, Bulvar Vernadskoho 36, 03142 Kyiv, Ukraine

(Received 24 November 2020, revised 31 March, accepted 7 April 2021)

Abstract: The electrical conductivity of solid solutions with tetragonal syngony formed in $0.86(xKF–(1–x)PbF_2)–1.14SnF_2$ systems has been studied by ^{19}F-NMR and impedance spectroscopy. It was found that the $Pb_{0.86}Sn_{1.14}F_4$ phase is characterized by better values of fluoride-ion conductivity than the β-$PbSnF_4$ compound. It was found that the substitution of Pb^{2+} by K^+ up to $x = 0.07$ in the structure of $Pb_{0.86}Sn_{1.14}F_4$ contributes to increase in electrical conductivity by an order of magnitude relative to the original $Pb_{0.86}Sn_{1.14}F_4$. The sample of composition $K_{0.03}Pb_{0.83}Sn_{1.14}F_{3.97}$ has the highest electrical conductivity (σ_{600} = = 0.38 S cm^{-1}, σ_{330} = 0.01 S cm^{-1}). The fluoride anions in the synthesized samples of $K_xPb_{0.86-x}Sn_{1.14}F_{4-x}$ solid solutions occupy three structurally non-equivalent positions. It is shown that with increasing temperature, there is a redistribution of fluorine anions between positions in the anion lattice, which results in an increase in the concentration of highly mobile fluoride ions, which determine the electrical conductivity of the samples.

Keywords: solid electrolytes; lead and tin fluorides; heterovalent substitution; impedance spectroscopy; ^{19}F-NMR spectroscopy.

INTRODUCTION

Fluoride-conducting compounds in the solid state have the potential to be used in electrochemical devices,[1–3] such as sensors,[4–6] ion-selective electrodes,[7,8] primary and secondary fluoride ion batteries, *etc.*[3,9] The effective usage of these devices depends on the right choice of electrode and electrolyte materials, the combination of which ensures rapid charge transfer by fluorine anions at the electrode–electrolyte interface. According to expert estimates, the theoretical specific energy of electrochemical power sources of this type can reach about 5 kWh dm^{-3} depending on the combination of electrode and electrolyte

* Corresponding author. E-mail: pogorenkoyulija@gmail.com
https://doi.org/10.2298/JSC201124031P

materials.[10–12] Fluoride ion conducting phases with mixed ion–electronic conductivity,[12] which contain compounds of metals that are able to reversibly change the oxidation state, promise much as electrode materials. Electrolyte materials must ensure a high rate of charge (fluoride ion) transport. In view of this, much attention has been paid to the search for new compounds with high unipolar fluoride ion conductivity, with the fluoride ions retaining their composition and structure over a wide temperature range.

Complex fluorides of bivalent metals (Ca, Ba, Mg, Pb, Sn) and trivalent metals (Y, Sm, Nd, Ce, La), the lattice of which correspond to the fluorite or tysonite structural type, are attractive in this respect.[1,13,14] The fluorides of the above elements are prone to form isovalent or aliovalent substitution solid solutions with the retention of original structural type over a wide temperature range, which contributes to increase in the concentration of defects (interstitial ions, vacancies, *etc.*) in the lattice and hence to an improvement of the conduction properties.

Aliovalent substitution solid solutions based on $PbSnF_4$ and $BaSnF_4$ fluorides are the subject of much attention. At as low as room temperature, they are characterized by high values of unipolar conductivity (10^{-2}–10^{-5} S cm^{-1}), which is provided by fluoride anions.[15–18] As of today, the effect of substitution of a part of the lead cations by trivalent metal cations on the conductivity of $PbSnF_4$ has been fairly thoroughly studied.[19] For instance, it was found that when up to 20 mol. % Pb^{2+} is substituted by Ln^{3+} (Ln = Y, La, Ce, Nd, Sm, Gd) in the $PbSnF_4$ structure, the electrical conductivity of the solid solutions formed in these cases are much higher compared with original $PbSnF_4$. The solid solutions containing 10.0–15.0 mol. % LnF_3 have the maximum conductivity.[20,21]

The substitution of a part of the lead ions by potassium ions contributes to increase in electrical conductivity relative to β-$PbSnF_4$. The samples of the composition $K_{0.10}Pb_{0.90}SnF_{3.90}$ has the highest conductivity and the lowest conductivity activation energy in the high-temperature region (σ_{573} = 0.13 S cm^{-1}).[22]

Despite the large body of accumulated experimental data on the effect of aliovalent substituents, including potassium ions, on the conduction properties of $PbSnF_4$-based complex fluorides,[15–22] the effect of different degrees of substitution of a part of the Pb^{2+} or Sn^{2+} by potassium ions on the properties of the fluoride ion conducting phases in the KF–PbF_2–SnF_2 system has not been unambiguously established. The effect of aliovalent substitution on the conductivity of complex lead and tin fluorides with nonstoichiometric ratio has been scantily studied. The aim of this study was to determine the effect of the substitution of Pb^{2+} or Sn^{2+} by K^+ on the electrical conductivity of the fluoride ion conducting phase $Pb_{0.86}Sn_{1.14}F_4$ with β-$PbSnF_4$ structure.

EXPERIMENTAL

Polycrystalline research samples were synthesized by melting together KHF_2, PbF_2 and SnF_2 at a temperature in the range 773–823 K in an argon atmosphere. Pre-dried and ground KHF_2, PbF_2 and SnF_2 were melted together in a platinum crucible in an argon atmosphere at 773 K, held at this temperature for 15 min and cooled with the furnace switched off (cooling rate of 3–5 K min^{-1}).

X-Ray diffraction (XRD) analysis of the synthesized samples was performed on a DRON-3M diffractometer with Cu$K\alpha$ radiation in the angle range of 10–80° with a step of 0.04° and an exposure time of 3 s at each point. To interpret the diffractograms, the study of the elemental composition of the obtained samples was performed using a scanning electron microscope equipped with an energy-dispersive spectrometer AZtecOne with an X-MaxN20 detector.

The conductivity of the synthesized samples was studied by impedance spectroscopy using an Autolab electrochemical module (Ekochemie) and a frequency response analyzer in the frequency range of 10^{-1}–10^{6} Hz (at an amplitude of initial signal of 10 mV). Pressed cylindrical samples 8 mm in diameter and 2.0–3.0 mm in thickness were used for the research. Polished platinum plates served as current leads to the samples under investigation.

The temperature dependence of conductivity was studied in the range of frequencies where it is not affected by polarization and relaxation effects. The measurements were made under cooling conditions in a range of 298–773 (±2) K after thermostating for 20–30 min in an argon atmosphere.

The electrical conductivity was calculated from the equation $\sigma = l/(sR)$, where l is the thickness of disk-shaped sample, s is contact area, R is ohmic resistance, which was determined from the results of impedance spectroscopy by the procedure described in the literature.[19,20]

The ^{19}F-NMR spectra were recorded on a Bruker Avance 400 spectrometer (frequency 376 MHz) in the temperature range of 150–453 (±2) K. The chemical shift (δ / ppm) was measured against a C_6F_6 standard with an accuracy of 1 ppm. The line width (at half height, ΔH) was determined in kHz with an error of not over 1 %.

RESULTS AND DISCUSSION

X-Ray phase analysis and EDS analysis

Samples of solid solutions $K_xPb_{0.86-x}Sn_{1.14}F_{4-x}$ (x = 0.03; 0.05; 0.07; 0.10; 0.15) were synthesized for the research. The composition of the formed phases was monitored by energy dispersive X-ray analysis (EDS). It was found that the content of elements in the synthesized samples with increasing potassium concentration approach the amount of the actually taken salts for the synthesis (Table I).

An analysis of the results of X-ray phase studies showed that the diffraction patterns of all synthesized samples show the same reflection as for $PbSnF_4$ tetragonal structure (JCPDS card No. 35-1086, Fig. 1). No reflections that would indicate the presence of phases of the original components were detected. Only on the diffraction spectrum of the solid solution $K_{0.15}Pb_{0.71}Sn_{1.14}F_{3.85}$ was the formation of an additional peak at an angle of 27.39° observed, which corresponds to the KF phase.

TABLE I. Atomic content (at. %) in the solid solutions

Sample	Element			
	K	Pb	Sn	F
$K_{0.03}Pb_{0.83}Sn_{1.14}F_{3.97}$	0.61	13.54	18.70	67.15
$K_{0.05}Pb_{0.81}Sn_{1.14}F_{3.95}$	0.94	13.09	18.59	67.38
$K_{0.07}Pb_{0.79}Sn_{1.14}F_{3.93}$	1.30	12.97	19.21	66.52

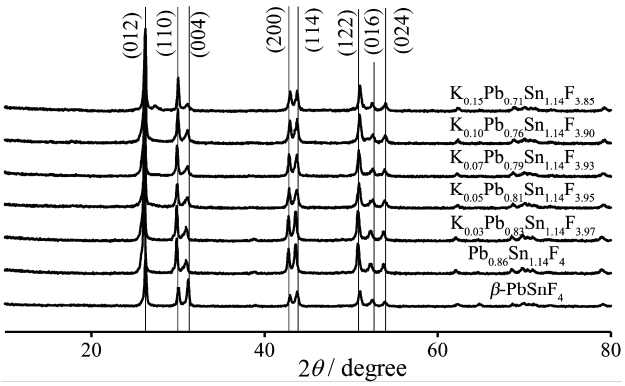

Fig. 1. X-Ray diffraction patterns of the synthesized samples.

According to the main peaks of the reference card (JCPDS card No. 35-1086), which are presented in Fig. 1, the values of the parameters of the crystal cells of the obtained solid solutions were calculated using the program UnitCell (Table II).

TABLE II. Lattice cell parameters (*a*, *c*, *V*) of the solid solutions $K_xPb_{0.86-x}Sn_{1.14}F_{4-x}$

Sample	*a* (±0.0006) / nm	*c* (±0.0023) / nm	*V* (±0.060) / nm^3
β-$PbSnF_4$	0.42132	1.15004	0.204147
$Pb_{0.86}Sn_{1.14}F_4$	0.42295	1.15518	0.206647
$K_{0.03}Pb_{0.83}Sn_{1.14}F_{3.97}$	0.42267	1.15608	0.206528
$K_{0.05}Pb_{0.81}Sn_{1.14}F_{3.95}$	0.42218	1.15164	0.205264
$K_{0.07}Pb_{0.79}Sn_{1.14}F_{3.93}$	0.42223	1.15103	0.205207
$K_{0.10}Pb_{0.76}Sn_{1.14}F_{3.90}$	0.42154	1.15089	0.204484
$K_{0.15}Pb_{0.71}Sn_{1.14}F_{3.85}$	0.42115	1.15097	0.204149
$PbSnF_4$ (JCPDS card No. 35-1086)	0.4216	1.1407	0.20276

It is noted that when a part of the Pb^{2+} are replaced by K^+ in the structure of the initial compound $Pb_{0.86}Sn_{1.14}F_4$, the parameters of the crystal lattice decrease with increasing KF content (Table II). This effect does not contradict the Goldschmidt rule and may be a consequence of the different polarity of the K–F and Pb–F bonds, as well as the structural features of $PbSnF_4$.[23] In addition, the distances Pb–F, Sn–F and the localization sites of fluorides were calculated based on the results of an X-ray diffraction analysis of a single crystal.[24] These dis-

tances indicate that K^+ can occupy the position of Pb^{2+} in the crystal lattice of $PbSnF_4$ without distortion of the unit cell.

Impedance spectroscopy

An analysis of the results of impedance studies showed that in the Nyquist coordinates (Fig. 2), the impedance hodographs of all investigated samples in the high-frequency region are represented by one deformed half-ring, which transforms, on transition to the low-frequency region, into a dependence, which characterizes polarization processes at the electrolyte/blocking electrode interface.[25] With increasing temperature, the radius of the deformed half-rings decreases (Fig. 2), and they shift to the higher-frequency region. This nature of change in impedance diagrams is typical of polycrystalline ion-conducting electrolytes with structural and energetic nonequivalence of charge carriers, fluorine anions.[26]

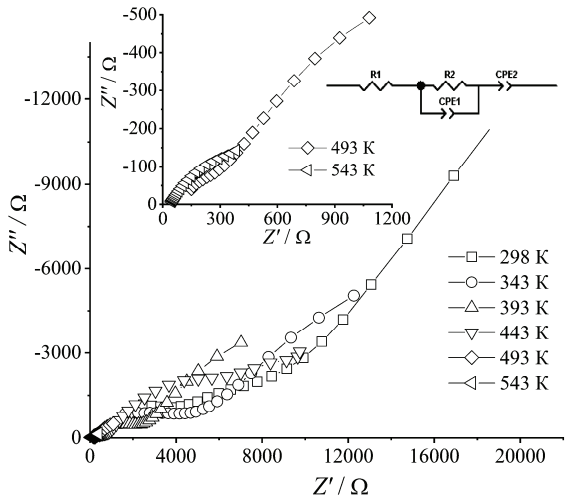

Fig. 2. Impedance hodographs and equivalent circuit of a polycrystalline sample of a $K_{0.03}Pb_{0.83}Sn_{1.14}F_{3.97}$ solid solution at different temperatures.

In all the cases the experimental complex impedance plot comprises a depressed semicircle accompanied by a straight line on the low frequency side, suggesting electrolyte–electrode polarization at the blocking electrodes. Such depression of the semicircle may originate from the presence of a distribution in relaxation times within the bulk response.[27,28] The radius of the semicircle decreases with increasing temperature due to the increase in the conductivity of the sample. The physical model (equivalent circuit) appropriate to these plots is shown in the inset of Fig. 2.

The equivalent circuit consists of a elements R1, acting as the bulk resistance a blocking layer capacitance in series with the parallel combination of bulk resistance (R2) and constant phase element (CPE1), where CPE is generally con-

sidered as a leaky capacitor (*i.e.*, hybrid between a resistor and a capacitor). Ideally the impedance assembly for solid electrolytes related to the process of charge transport in the bulk specimen is represented by parallel combination of R_b and C_b, where R_b represents the bulk resistance and capacitance C_b arises due to the electric relaxation process.[29] However, in this case C_b was replaced by CPE1, which accounts for the observed depression of the semicircle, and also the non-ideal electrolyte symmetry CPE2 in the equivalent circuit accounts for the formation of inclined straight line in the low frequency region.

In the low-frequency region, resistance values associated with the polarization of near-electrode layers of solid electrolytes are recorded. As a rule, they are higher, the lower the frequency and the higher the temperature. In the frequency range of 0.1–100 kHz, frequency-independent values were recorded. They coincide with the conductivity values calculated from the values of the resistance R_2 of the equivalent circuit and the results of measurement by the bridge method at frequencies of 10–70 kHz; therefore, they were used in the analysis of plots of electrical conductivity *versus* temperature, $\sigma = l/sR_2$.

The plots of electrical conductivity *versus* temperature (Fig. 3, Table III) for all synthesized and investigated samples of solid solutions $K_xPb_{0.86-x}Sn_{1.14}F_{4-x}$ can be arbitrarily divided into two region: the low-temperature and the high-temperature regions. The transition between them is observed in the temperature range 340–430 K. Both in the high-temperature region and in the low-temperature region, these plots are satisfactorily approximated by the Arrhenius–Frenkel equation (straight line in the $\log \sigma - 1000T^{-1}$ coordinates).

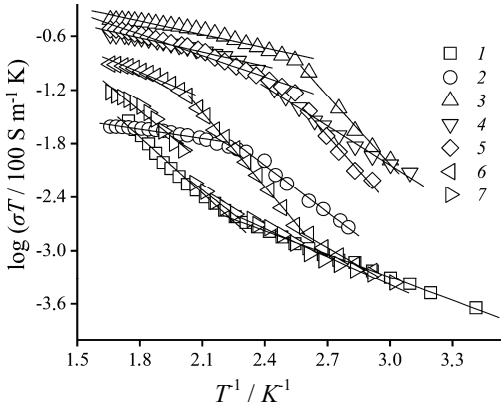

Fig. 3. Plots of electrical conductivity *versus* temperature for polycrystalline samples of $K_xPb_{0.86-x}Sn_{1.14}F_{4-x}$ solid solutions: 1: β-$PbSnF_4$; 2: $Pb_{0.86}Sn_{1.14}F_4$; 3: $x = 0.03$; 4: $x = 0.05$; 5: $x = 0.07$; 6: $x = 0.1$; 7: $x = 0.15$.

The increase in electrical conductivity in the sample $Pb_{0.86}Sn_{1.14}F_4$ in comparison with the sample $PbSnF_4$ is due to the fact that the interstitial fluorine anions (position F3) are coordinated around the cations Sn^{2+}. This is evidenced by the results of the publication, which shows that the anions in position F3 (tetrahedra) are coordinated in the planes of the cationic lattice, where the cations

were Sn^{2+}.[24] Increasing the concentration of tin cations contributes to the increase of interstitial anions.

TABLE III. Electrical conductivity parameters of the solid solutions $K_xPb_{0.86-x}Sn_{1.14}F_{4-x}$

Sample	ΔE_a (± 0.02) / eV	log (A / S cm^{-1} K^{-1})	σ / S cm^{-1}	T / K
β-$PbSnF_4$	0.36	4.19	$9.02\cdot10^{-4}$ (373)	298–373
	0.20	2.27	$1.88\cdot10^{-2}$(573)	383–623
$Pb_{0.86}Sn_{1.14}F_4$	0.28	9.06	$2.9\cdot10^{-3}$ (373)	298–420
	0.18	6.67	$1.75\cdot10^{-2}$ (473)	430–480
	0.08	4.64	$2.41\cdot10^{-2}$ (573)	490–623
$K_{0.03}Pb_{0.83}Sn_{1.14}F_{3.97}$	0.49	18.24	0.12 (373)	298–370
	0.19	9.57	0.287 (473)	380–450
	0.09	7.58	0.373 (573)	460–623
$K_{0.05}Pb_{0.81}Sn_{1.14}F_{3.95}$	0.23	9.32	$2.29\cdot10^{-2}$ (373)	298–430
	0.14	7.92	0.25(573)	440–623
$K_{0.07}Pb_{0.79}Sn_{1.14}F_{3.93}$	0.53	18.63	$1.93\cdot10^{-2}$ (373)	298–370
	0.23	10.20	0.167 (473)	380–460
	0.15	8.25	0.279(573)	470–623
$K_{0.10}Pb_{0.76}Sn_{1.14}F_{3.90}$	0.33	9.53	$1.08\cdot10^{-3}$ (373)	298–400
	0.52	15.45	$2.65\cdot10^{-2}$ (473)	410–510
	0.17	8.51	0.11 (573)	520–623
$K_{0.15}Pb_{0.71}Sn_{1.14}F_{3.85}$	0.26	7.11	$7.85\cdot10^{-4}$(373)	298–430
	0.75	19.09	$4.58\cdot10^{-3}$(473)	470–540
	0.25	9.06	$4.94\cdot10^{-2}$ (573)	550–623

The influence of tin cations on the electrical conductivity of samples of the PbF_2–SnF_2 system is evidenced by the results of previous studies.[30] In these works, it was shown that the replacement of part of Pb^{2+} by Sn^{2+} increases the electrical conductivity and significantly reduces the activation energy.

The slight substitution (x = 0.03) of Pb^{2+} by K^+ in the $Pb_{0.86}Sn_{1.14}F_4$ structure causes an increase in electrical conductivity: at 600 K, its value is 0.38 S cm^{-1} and at 330 K 0.01 S cm^{-1}, which is an order of magnitude higher compared with original $Pb_{0.86}Sn_{1.14}F_4$ and two orders of magnitude higher compared to pure β-$PbSnF_4$ (Fig. 4A). In this case, the conductivity activation energy in the high-temperature region does not practically change (0.08 eV for original $Pb_{0.86}Sn_{1.14}F_4$ and 0.09 eV for $Pb_{0.83}K_{0.03}Sn_{1.14}F_{3.97}$ solid solution), and the total electrical conductivity increases owing to the appearance of vacancies in the anion sublattice (Fig. 4B).

When the K^+ content further increases (to x = 0.07), the fluoride ion conductivity of samples slightly decreases over the entire temperature range (Table III). The temperature dependence of the electrical conductivity of the solid solution of composition $K_{0.15}Pb_{0.71}Sn_{1.14}F_{3.85}$ is similar to that of β-$PbSnF_4$; in the high-temperature region, however, its values are somewhat higher and comparable with those of $PbSnF_4$ at temperatures below 490 K.

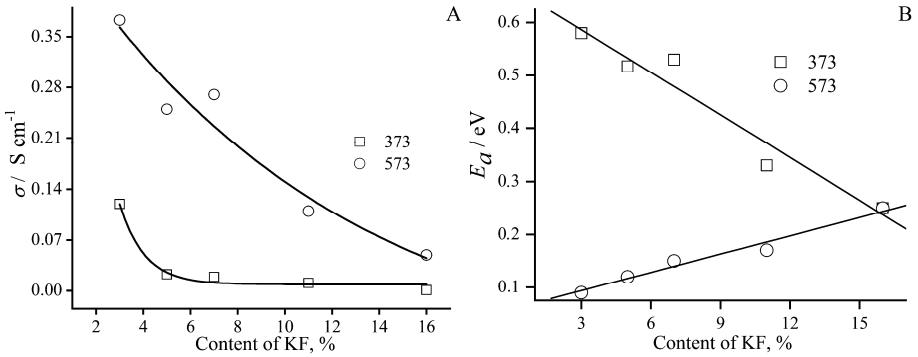

Fig. 4. Plots of electrical conductivity (A) and activation energy (B) *versus* potassium fluoride content for $K_xPb_{0.86-x}Sn_{1.14}F_{4-x}$ samples.

The electrical conductivity of the synthesized samples with the percentage of potassium ions replacing Pb^{2+} of over $x = 0.03$ decreases over the entire temperature range (Fig. 4). Unlike the compounds with purely interstitial conduction mechanism, the activation energy for $K_xPb_{0.86-x}Sn_{1.14}F_{4-x}$ solid solutions at $T > 450$ K increases with potassium fluoride content.[20] This may be due to the fact that the motion of fluoride ions between vacant positions requires a higher expenditure of energy than that in interstitial spaces.

NMR spectroscopy

Important information on the nature of charge carries in the system under investigation was obtained by ^{19}F-NMR spectroscopy. Typical ^{19}F-NMR spectra for, as an example, a $K_{0.03}Pb_{0.83}Sn_{1.14}F_{3.97}$ solid solution are shown in Fig. 5. The width of the spectral bands is determined by the interaction of the nuclear magnetic moments of fluorine. The appearance of the obtained spectra indicates that the fluorine anions occupy structurally different positions in the lattice.[31,32]

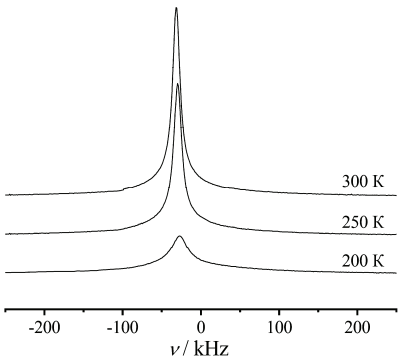

Fig. 5. ^{19}F-NMR spectra of a $K_{0.03}Pb_{0.83}Sn_{1.14}F_{3.97}$ solid solution at different temperatures.

Three position can be distinguished, F(1) in a rigid lattice with immobile anions, which are on triple axes, F(2) with locally mobile anions on the same

axes and F(3) interstitial fluorine anions. With increasing temperature, a redistribution of fluorine anions between the positions occupied by them in the lattice occurs.[31,32] The narrow spectral component characterizing highly mobile interstitial ions becomes predominant in the integrated intensity. This anions redistribution is inherent in the overwhelming majority of fluoride ion conducting phases with fluorite and tysonite structures.[32]

The transformation of the shape of the resonance band in the temperature range of 150–453 K entails a significant decrease in ΔH from 96 to 5 kHz (Fig. 6). The value of chemical shift at 150 K is ≈16 ppm and shifts to –31 ppm at 300 K. The chemical shift of the narrow component is sensitive to the type of structural positions occupied by ions in the diffusion process.

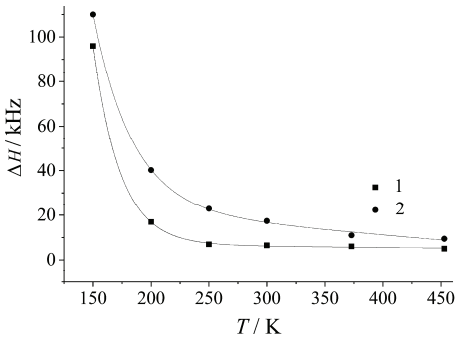

Fig. 6. Temperature dependence of the band width at half-height, ΔH(F), of the ^{19}F-NMR spectrum of a polycrystalline samples of solid solution: 1 – $K_{0.03}Pb_{0.83}Sn_{1.14}F_{3.97}$ and 2 – $K_{0.07}Pb_{0.79}Sn_{1.14}F_{3.93}$.

If the movement occurs only at positions of one type, then the chemical shifts of the "rigid" and narrow components must remain constant and should not depend on temperature. In the case when the ion visits other structural positions during diffusion, the shift of the narrow line will depend on temperature and can be represented by the average value $\langle\delta\rangle = \sum p_k\delta_k$, where p_k and δ_k are the mass coefficient and chemical shift of the k-th structural position.

The decomposition of the ^{19}F-NMR spectra of synthesized samples into components characterizing certain positions of fluorine anions in the lattice (Fig. 7) was performed according to Gabuda, *et a.l*[33] and Kavun *et al.*[34]

Since the area of the spectral components is proportional to the amount of fluorine anions, which are in one position or another, their fraction in the structure of the fluoride ion conducting phase at different temperatures can be quantitatively estimated in a first approximation. For instance, the fraction of the "highly mobile" fluorine anions that are in the interstitial spaces of the lattice (position F(3), spectral component P_3) at 150 K is not over 26 % and increases with rising temperature to 63 % at 300 K and 87 % at 453 K owing to drawing in fluoride ions from the locally mobile position F(2) and immobile position F(1) (Fig. 8). As can be seen from the presented data, up to 270 K, mainly the amount of anions that are position F(2) (the area of spectral component P_2) decreases.

The amount of fluorine anions that are in position F(1) (the area of spectral component P_1) does not practically change. At higher temperatures, they also move to interstitial positions F(3).

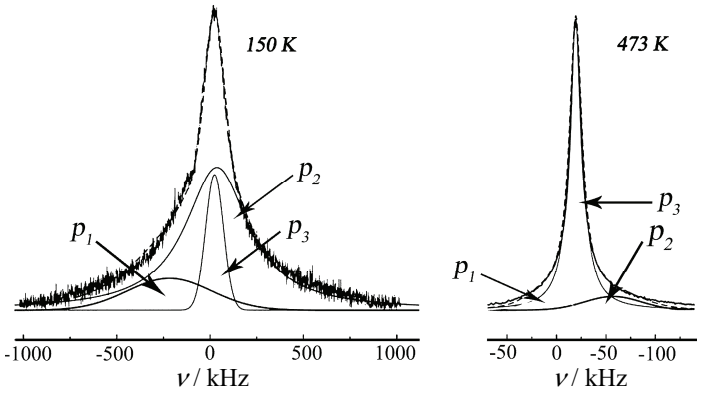

Fig. 7. Transformation of ^{19}F-NMR spectra and their components of $K_{0.03}Pb_{0.83}Sn_{1.14}F_{3.97}$ solid solutions with rising temperature.

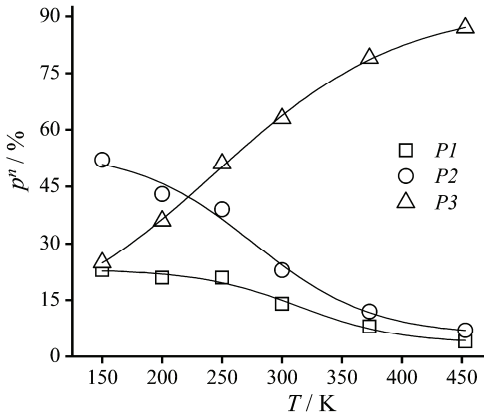

Fig. 8. Fluoride anion distribution over localization sites in the lattice of $K_{0.03}Pb_{0.83}Sn_{1.14}F_{3.97}$ at different temperatures.

The results of the NMR study agree with the trend of plots of conductivity *versus* temperature for the compounds $K_xPb_{0.86-x}Sn_{1.14}F_{4-x}$. For instance, the $\log \sigma - 1000T^{-1}$ plots for each sample exhibit a kink in the temperature range of 370–430 K, which is characteristic of most solid electrolytes with fluorite and antifluorite structures. Such dependence of electrical conductivity of temperature in the scientific literature is described as "Faraday phase transition".[35] Its appearance is considered to be caused by an increase in the concentration of fluoride anions in the intermediate spaces of the crystal lattice when heated and their rate of migration.[14,36] It is well known that in fluorine conducting the phases of fluorite and tysonite structures, the fluoride anions occupy three different positions, differing from each other by the local medium of the cation and the bond length M–F.[37] At a

certain temperature T_k, locally mobile fluorine anions acquire energy sufficient to overcome the energy barrier and move into the interstitial cavities. This is also largely due to the thermal fluctuations of lead and tin cations.

Approximately in this temperature range, the width at half-height of the bands in NMR spectra reaches minimum values (≈5 kHz), and the fluorines occupy mobile positions F(3).

CONCLUSIONS

The partial substitution of lead ions by potassium cations in the fluoride ion conducting phase of composition $Pb_{0.86}Sn_{1.14}F_4$ with a β-$PbSnF_4$ structure causes an increase of almost an order of magnitude in electrical conductivity relative to original β-$PbSnF_4$. On substitution, fluoride ion conducting phases $K_xPb_{0.86-x}Sn_{1.14}F_{4-x}$ (x = 0.03; 0.05; 0.07; 0.10; 0.15) isostructural to β-$PbSnF_4$ are formed, the lattice of which corresponds to tetragonal syngony.

The light substitution of Pb^{2+} by potassium ions (up to x = 0.07 inclusive) in the fluoride ion conducting $Pb_{0.86}Sn_{1.14}F_4$ phase causes an increase in electrical conductivity over the entire studied temperature range. The sample of the composition $K_{0.03}Pb_{0.83}Sn_{1.14}F_{3.97}$ has the highest electrical conductivity (σ_{600} = 0.38 S cm^{-1}, σ_{330} = 0.01 S cm^{-1}). When the amount of substituent is further increased, the electrical conductivity in the low-temperature region decreases.

The conductivity of the synthesized solid electrolytes is provided by interstitial fluoride anions. Increasing the temperature contributes to an increase in their concentration and, as a result, in the conductivity of the solid solutions. At temperatures above 400 K, most of the fluorine ions (over 90 %) of the synthesized fluoride ion conducting phases are in highly mobile (interstitial) positions in the lattice.

Acknowledgement. This work was realized within the state project No. 0119U001824 with the financial support of MES of Ukraine.

ИЗВОД

ПРОВОДЉИВОСТ ФЛУОРИДНИХ ЈОНА ЧВРСТОГ РАСТВОРА KXPB0.86-XSN1.14F4-X

YULIIA POHORENKO[1], ROMAN PSHENYCHNYI[2], TAMARA PAVLENKO[1], ANATOLIY OMEL'CHUK[1] и VOLODYMYR TRACHEVSKYI[3]

[1]V.I. Vernadskii Institute of General and Inorganic Chemistry of the Ukrainian NAS, 32–34 Acad. Palladina Ave., 03142 Kyiv, Ukraine, [2]Sumy State University, Rymskogo-Korsakova st. 2, 40007 Sumy, Ukraine и [3]G.V. Kurdyumov Institute of Metal Physics of the Ukrainian NAS, Bulvar Vernadskoho 36, 03142 Kyiv, Ukraine

Електрична проводљивост чврстих раствора са тетрагоналном сингонијом, формираних у систему $0{,}86(x\mathrm{KF}–(1–x)\mathrm{PbF_2})–1{,}14\mathrm{SnF_2}$, испитивана је методом ^{19}F-спектроскопије нуклеарне магнетне резонанације (^{19}F-NMR) и спектроскопијом електрохемијске импеданције. Нађено је да је проводљивост флуоридних јона у фази $Pb_{0,86}Sn_{1,14}F_4$ боља у поређењу са једињењем β-$PbSnF_4$. Такође је показано да замена Pb^{2+} јонима K^+ до удела x = 0,07 у структури $Pb_{0,86}Sn_{1,14}F_4$ доприноси повећању електричне

проводљивости за један ред величине у односу на првобитни $Pb_{0,86}Sn_{1,14}F_4$. Узорак састава $K_{0,03}Pb_{0,83}Sn_{1,14}F_{3,97}$ поседује највећу електричну прводљивост (σ_{600} = 0,38 S cm^{-1}, σ_{330} = 0,01 S cm^{-1}). Флуориди у синтетисаним узорцима чврстог раствора $K_xPb_{0,86-x}Sn_{1,14}F_{4-x}$ заузимају три структурно нееквивалентне позиције. Показано је да са повећањем температуре долази до прерасподеле флуоридних јона између места у анјонској решетки, што доводи до повећања концентрације високо покретљивих флуоридних јона, који одређују електричну проводљивост узорака.

(Примљено 24. новембра 2020, ревидирано 31. марта, прихваћено 7. априла 2021)

REFERENCES

1. V. Trnovcová, P. P. Fedorov, I. Furár, *Russ. J. Electrochem.* **45** (2009) 630 (https://doi.org/10.1134/S1023193509060020)
2. T. Nakajima, H. Groult, *Advanced Fluoride-Based Materials for Energy Conversion*, Elsevier, Amsterdam, 2015 (https://doi.org/10.1016/C2013-0-18650-3)
3. F. Gschwind, G. Rodriguez-Garcia, D. J. S. Sandbeck, A. Gross, M. Weil, M. Fichtner, N. Hörmann, *J. Fluorine Chem.* **182** (2016) 76 (https://doi.org/10.1016/j.jfluchem.2015.12.002)
4. J. W. Fergus, *Sensors Actuators, B* **42** (1997) 119 (https://doi.org/10.1016/S0925-4005(97)00193-7)
5. X. Na, W. Niu, H. Li, J. Xie, *Sensors Actuators, B* **87** (2002) 222 (https://doi.org/10.1016/S0925-4005(02)00238-1)
6. W. Moritz, S. Krause, U. Roth, J. Xie, *Anal. Chim. Acta* **437** (2001) 183
7. X. D. Wang, W. Shen, R. W. Cattrall, G. L. Nyberg, J. Lieseganget, *Aust. J. Chem.* **49** (1996) 897 (https://doi.org/10.1071/CH9960897)
8. M. Fouskaki, S. Sotiropoulou, M. Kosi, N. A. Chaniotakis, *Anal. Chim. Acta* **478** (2003) 77 (https://doi.org/10.1016/S0003-2670(02)01481-2)
9. L. Zhang, M. A. Reddy, M. Fichtner, *Solid State Ionics* **272** (2015) 39 (https://doi.org/10.1016/j.ssi.2014.12.010)
10. C. B. Alcock, L. Baozhen, *Solid State Ionics* **39** (1990) 245 (https://doi.org/10.1016/0167-2738(90)90403-E)
11. C. Rongeat, M.A. Reddy, R. Witter, M. Fichtner, *J. Phys. Chem.* **117** (2013) 4943 (https://doi.org/10.1021/jp3117825)
12. A. Potanin, *J. Russ. Chem. Soc.* **45** (2001) 58
13. L. N. Patro, K. Hariharan, *Solid State Ionics* **239** (2013) 41 (https://doi.org/10.1016/j.ssi.2013.03.009)
14. N. I. Sorokin, B. P. Sobolev, *Crystallogr. Rep.* **52** (2007) 842 (https://doi.org/10.1134/S1063774507050148)
15. N.I. Sorokin, *Inorg. Mater.* **40** (2004) 989 (https://doi.org/10.1023/B:INMA.0000041335.17098.d1)
16. N. I. Sorokin, P. P. Fedorov, B. P. Sobolev, *Inorg. Mater.* **33** (1997) 1
17. A. M. Vakulenko, E. A. Ukshe, *Sov. Electrochem.* **28** (1992) 1025.
18. P. P. Fedorov, V. K. Goncharuk, I. G. Maslennikova, I. A. Telin, T. Y. Glazunova, *Russ. J. Inorg. Chem.* **61** (2016) 239 (https://doi.org/10.1134/S0036023616020078)
19. R. Kanno, S. Nakamura, Y. Kawamoto, *Solid State Ionics* **51** (1992) 53 (https://doi.org/10.1016/0167-2738(92)90343-N)

20. Yu. V. Pohorenko, R. M. Pshenychnyi, A. O. Omelchuk, V. V. Trachevskyi, *Solid State Ionics* **338** (2019) 80 (https://doi.org/10.1016/j.ssi.2019.05.001)
21. Y. V. Pogorenko, R. M. Pshenichnyi, V. I. Lutsyk, A. O. Omel'chuk, *IOP Conf. Ser.: Mater. Sci. Eng.* **175** (2017) 012039 (https://doi.org/10.1088/1757-899X/175/1/012039)
22. Yu. V. Pohorenko, A. A. Nahorny, R. M. Pshenychnyi, A. O. Omel'chuk, *Voprosy Khim. Khim. Tekhnol.* **5** (2019) 112 (http://dx.doi.org/10.32434/0321-4095-2019-126-5-112-117)
23. V. M. Goldschmidt, *Naturwissenschaften* **14** (1926) 477 (https://doi.org/10.1007/BF01507527)
24. Y. Ito, T. Mukoyama, H. Funatomi, S. Yoshikado, T. Takana, *Solid State Ionics* **67** (1994) 301 (https://doi.org/10.1016/0167-2738(94)90021-3)
25. A. K. Jonscher, *Nature* **267** (1977) 673 (https://doi.org/10.1038/267673a0)
26. J. T. S. Irvine, D. C. Sinclair, A. R. West, *Adv. Mater.* **2** (1990) 132 (https://doi.org/10.1002/adma.19900020304)
27. M. El Omari, J. Senegas, J. M. Réau, *Solid State Ionics* **107** (1998) 281 (https://doi.org/10.1016/S0167-2738(97)00535-3)
28. M. M. Ahmad, K. Yamada, T. Okuda, *J. Phys. Condens. Matter.* **14** (2002) 7233 (https://iopscience.iop.org/article/10.1088/0953-8984/14/30/312)
29. E. Barsoukov, J. R. Macdonald, *Impedance spectroscopy emphasizing solid materials and systems*, John Wiley and Sons, Inc., Hoboken, NJ, 2005. (ISBN: 0-471-64749-7)
30. S. Vilminot, G. Perez, W. Granier, L. Cot, *Solid State Ionics* **2** (1981) 91 (https://doi.org/10.1016/0167-2738(81)90004-7)
31. M. G. Izosimova, A. I. Livshits, V. M. Buznik, P. P. Fedorov, E. A. Krivandina, B. P. Sobolev, *Sov. Phys.-Sol. State* **28** (1986) 2644.
32. V. Ya. Kavun, A. I. Ryabov, I. A. Telin, A. B. Podgorbunskii, S. L. Sinebryukhov, S. V. Gnedenkov, V.K. Goncharuk, *J. Struct. Chem.* **53** (2012) 290 (https://doi.org/10.1134/S0022476612020126)
33. S. P. Gabuda, Yu.V. Gagarinsky, S. A. Polishchuk, *NMR in inorganic fluorides, Atomizdat*, Moscow, 1978
34. V. Ya. Kavun, N. F. Uvarov, A. B. Slobodyuk, M. M. Polyantsev, A. S. Ulihin, E. B. Merkulov, V. K. Goncharuk, *Solid State Ionics* **330** (2019) 1 (https://doi.org/10.1016/j.ssi.2018.12.004)
35. D. P. Almond, A. R. West, *Solid State Ionics* **9**–**10** (1983) 277 (https://doi.org/10.1016/0167-2738(83)90247-3)
36. Sh. Yoshikado, Y. Ito, J. M. Réau, *Solid State Ionics* **154**–**155** (2002) 503 (https://doi.org/10.1016/S0167-2738(02)00489-7)
37. C. Martineau, F. Fayon, C. Legein, J. Y. Buzaré, G. Corbel, *Chem. Mater.* **22** (2010) 1585 (https://doi.org/10.1021/cm9030182).